Energy &
Environment Nexus

https://doi.org/10.48130/een-0026-0012

Original Research

Open Access

Combustion characteristics and thermokinetics of coal blended with organic cleaning wastewater

Jun Zhang, Yaji Huang*, Yizhuo Qiu, Xinyi Jiang, Lanpeng Zhang and Hao Shi

Received: 16 March 2026

Revised: 19 April 2026

Accepted: 8 June 2026

Published online: 30 June 2026

Abstract

This study investigates the combustion characteristics and thermokinetic behavior of bituminous coal blended with 1–10 wt% organic cleaning wastewater (OCW) using non-isothermal thermogravimetric analysis. The addition of OCW reduced the ignition temperature from 411.6 to 392.4 °C and slightly lowered the maximum and mean mass-loss rates by introducing moisture- and acid-driven endothermic effects. The comprehensive combustion index decreased by 4%–15% with increasing OCW ratio, indicating suppressed global reactivity. Kinetic analysis based on Flynn–Wall–Ozawa and Kissinger–Akahira–Sunose methods revealed a reduction in apparent activation energy by 8–15 kJ·mol^{-1} at 1–5 wt% OCW due to catalytic effects of oxygen-containing organics and Fe/Na species. At 10 wt% OCW, burnout temperature increased, and the S decline intensified because of heat-absorption dilution and ash-induced diffusion resistance. The novelty of this work lies in systematically revealing the coupled promotion–inhibition effects of OCW on coal combustion through the combined analysis of combustion characteristic indices. The result provides a scientific basis for the co-disposal of chemical cleaning wastewater in pulverized coal-fired boilers.

Keywords: Coal combustion, Organic cleaning wastewater, TGA, Kinetic analysis

Highlights

- Adding 1–5 wt% of OCW lowers coal's ignition temperature via catalysis.
- OCW addition slightly suppresses overall combustion reactivity due to its moisture and acidic content.
- At 10 wt%, high moisture and ash in OCW negatively impact combustion performance.
- Investigating the effects of OCW on pulverized coal combustion to provide reference for utilizing OCW in pulverized coal boilers.

Graphical abstract

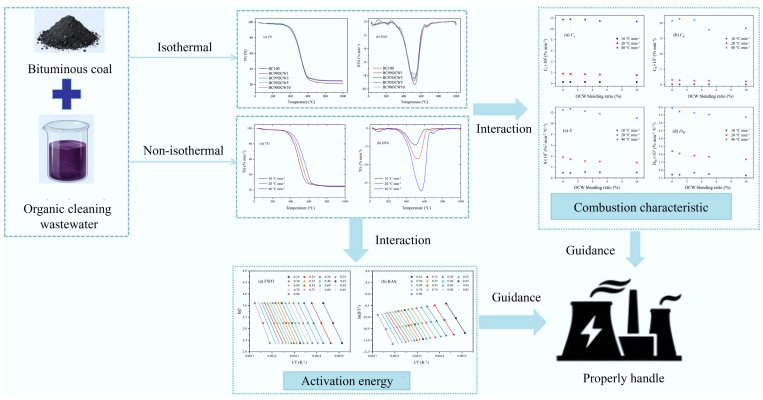

* Correspondence: Yaji Huang (heyyj@seu.edu.cn)

Full list of author information is available at the end of the article.

https://doi.org/10.48130/een-0026-0012

Introduction

Chemical cleaning technology is widely used in industrial fields such as power generation, petrochemical industry, oil and gas operation, and heat exchange systems, and is used to remove scale, corrosive products, and organic sediments on equipment surfaces, pipelines, and key process components[1]. Among the commonly used cleaning agents, ethylenediaminetetraacetic acid (EDTA) and citric acid are widely used in the maintenance of boilers and various infrastructures because of their strong chelation ability and high cleaning properties. However, the use of these reagents will inevitably produce a large amount of wastewater, which contains a high concentration of chemical oxygen demand (COD), a variety of complex organic compounds, and a large amount of heavy metal ions released during each cleaning cycle[2,3]. In addition, to improve cleaning efficiency and protect the surface of equipment, it is often necessary to add anionic and non-ionic surfactants, corrosion inhibitors, and auxiliary additives, which further aggravates the environmental burden of wastewater flow. According to The National Directory of Hazardous Waste (2025), chemical cleaning wastewater is classified as hazardous waste and must be treated in a standardized and safe manner.

In order to address this challenge, a variety of treatment technologies have been developed for the disposal of organic cleaning wastewater (OCW). Biological treatment processes such as denitrification and aerobic or anaerobic degradation can effectively remove nitrogen-containing pollutants and biodegradable organic matter[4–6]. Physical and chemical methods—including the use of active materials or ion exchange resins for adsorption—can selectively capture heavy metal ions and reduce acid consumption in practical applications[7,8]. Chemical oxidation methods based on electrochemical reactions, advanced oxidation processes, and catalytic oxidation also exhibit high COD removal efficiency. Many studies have shown that the COD degradation rate can exceed 90% under optimized conditions[9–11]. Zeng et al.[12] achieved a removal rate of more than 99% of nitrate and total nitrogen in the denitrification reactor, while Tong et al.[3] achieved a COD removal efficiency of 94.63% using an electrochemical system. Although these methods are effective, they often require complex infrastructure and high operating costs, and may also produce derived pollutants that need secondary treatment.

Compared with traditional treatment methods, incineration provides an efficient and stable chemical oxidation route, which can completely mineralize organic matter into carbon dioxide and water. A variety of incineration technologies, including liquid flow incineration, rotary kiln incineration, immersion thermal plasma, and fluidized bed systems, have been widely studied and applied to the destruction of organic waste liquid[13–15]. Mabrouk et al.[16] confirmed that immersion thermal plasma technology can maintain a total organic carbon destruction efficiency exceeding 99% when treating different wastes. In addition, pretreatment strategies such as drying or concentration can further improve combustion performance and reduce the emission of incomplete combustion products[17]. Yang et al.[14] revealed that in the process of pyrolysis and combustion of wastewater with high water content, raising the incineration temperature from 900 to 1,000 °C can reduce nitrogen oxide emissions, highlighting the importance of combustion conditions.

Yang et al.[18] directly investigated the co-combustion behavior of organic waste liquid and pulverized coal in 2025. Thermogravimetric analysis, Fourier-transform infrared spectroscopy, and gas chromatography–mass spectrometry were employed to analyze the co-combustion characteristics and gaseous products. The results demonstrated a pronounced synergistic effect between the organic waste liquid and pulverized coal. An appropriate blending ratio of organic waste liquid promoted volatile release and improved combustion stability, whereas an excessively high blending ratio led to incomplete combustion and increased CO emissions. In terms of engineering applications, as early as the 1990s, Wangting Power Plant conducted engineering practice on the disposal of citric acid waste liquid by utilizing the high-temperature environment of a coal-fired boiler. This work verified the feasibility of harmless disposal of organic waste liquid in pulverized coal furnaces under conditions of high temperature and intense turbulence, thereby providing an important engineering foundation for the subsequent development of technologies for the co-disposal of organic waste liquid in pulverized coal boilers[19]. Chen[20], focusing on EDTA waste liquid generated from the chemical cleaning of boilers in thermal power plants, proposed a treatment method in which the waste liquid was sprayed onto coal piles or coal-conveying belts, adsorbed by the coal, and then fed into the furnace together with the coal for incineration. When the daily spray volume was controlled at approximately 20 t, this process enabled effective disposal of the waste liquid without significantly affecting boiler combustion stability. After spraying, the total moisture content of the as-fired coal increased from 14.49% to 17.46%; however, the combustible content in fly ash and bottom slag decreased by 0.27 and 6.71 percentage points, respectively, indicating that combustion performance was not adversely affected. The dust concentration in the flue gas at the inlet of the flue gas desulfurization unit decreased from 74.13 to 36.90 mg·m^{-3}, and the pollutant concentrations at the outlet also complied with the relevant emission standards. Despite these advances, OCW still has the characteristics of extremely high moisture content, low calorific value, and the presence of thermally stable complexes such as ethylenediaminetetraacetic acid–metal chelates, making it unsuitable for use as an independent fuel. Therefore, co-combustion with pulverized coal in existing coal-fired boilers has become a promising alternative. This cooperative treatment strategy has multiple advantages: (i) using the existing high-temperature combustion environment without additional treatment facilities; (ii) realizing heat recovery and pollutant destruction synchronously; (iii) providing cost-effective and easy-to-operate solutions for power plants seeking to reduce hazardous waste emissions. However, after organic wastewater is introduced into the coal-fired system, it may affect the ignition behavior, volatile release, combustion characteristics, and reaction kinetics of the combustion system due to factors such as the dilution effect, metal ion catalytic activity, and organic acid heat decomposition. So far, the research on the combustion characteristics and kinetic behavior of organic wastewater when directly mixed with coal is still relatively limited.

Therefore, the main goal of this study is to systematically explore the impact of low-ratio OCW addition on the combustion characteristics of pulverized coal at different heating rates. By analyzing the ignition temperature, burnout behavior, mass loss dynamics, and dynamic parameters, it aims to clarify how OCW affects the overall combustion process. The research results provide basic data and a scientific basis for the collaborative treatment of OCW by coal-fired boilers, and provide practical references for industrial practical application and environmental management.

Experiments and analysis

Materials

The bituminous coal (BC) was collected from the Dalyu coal mine (Shaanxi Province, China); the OCW was collected from BaoSteel in

Shanghai, China. Before the test, the coal was dried in an oven at 105 °C for 24 h. The dried coal was put into a sieve and shaken by an electric vibrating sieve separator, then the coal of 100–150 mesh (0.1–0.15 mm) was taken out and bottled. The coal sample was divided into five parts to prepare different mass ratio OCW samples. The sample without adding OCW was marked as BC100. OCW was added to the samples and then fully mixed using a glass rod. In this study, the additions of OCW were 1, 3, 5, and 10 wt%, respectively. And BC(100-n)OCWn was used to represent different mixed samples.

According to GB/T 212–2001, similar analysis and limit value analysis were carried out on the coal. The conclusion is shown in Table 1.

Organic chemical cleaning demonstrates superior efficacy under alkaline conditions. Ammonia solution was employed to adjust the pH of the organic chemical cleaning agent, resulting in an OCW pH of 9.35 with substantial NH_3-N content. The primary constituent of this organic chemical cleaning agent is disodium EDTA. By utilizing EDTA's chelating capacity to remove iron salts and other components from scale deposits, the OCW contained significant quantities of Fe and Na elements, presenting a deep purple colouration. The quality of OCW is shown in Table 2.

Thermogravimetry analysis

Combustion characteristics of coal and their mixtures were analyzed in TGA experiments using a simultaneous thermal analyzer (STA 449F5, temperature stability 0.1 °C) manufactured by Netzsch. In each run, 5 ± 1 mg of sample was placed in a corundum crucible and spread evenly. The samples were heated at a rate of 20 °C·min^{-1} between 30 and 1,000 °C to ensure complete combustion of the fuel in purged nitrogen and air at a flow rate of 50 mL·min^{-1}. Weight loss vs temperature was recorded in real time by computer software with a temperature accuracy of 0.1 °C. Prior to the experiment, three randomly selected samples of each type were dried in a forced-air oven at 105 °C to constant weight to ensure that the deviation of the actual OCW content from the preset blending ratio did not exceed 0.5%.

Combustion parameters

Characteristic temperatures, such as ignition temperature (T_i, °C), burnout temperature (T_b, °C), and peak temperature (T_p, °C), were directly extracted from TGA-DTG curves to evaluate combustion behavior. Among them, T_i was identified using the tangent method. Specifically, the ignition temperature is defined as the intersection temperature between the baseline and the tangent line derived at the point of maximum mass loss rate on the TG profile. T_p and T_b represent the temperatures at which the maximum mass loss rate occurs, and the fuel conversion reaches 98%, respectively[21].

In this study, the combustion performance of the sample was evaluated based on several key parameters, including the comprehensive combustion characteristics index (S, %^{2}·min^{-2}·°C^{-3}), the ignition index (C_i, %·min^{-3}), the burnout index (C_b, %·min^{-4}), and the burning stability index (D_W, %·min^{-1}·°C^{-2})[22,23]. These indices are defined as follows:

$$C_i = \frac{\left(\frac{dw}{dt}\right)_{max}}{t_i t_p} \quad (1)$$

$$C_b = \frac{\left(\frac{dw}{dt}\right)_{max}}{t_{1/2} t_p t_b} \quad (2)$$

$$S = \frac{\left(\frac{dw}{dt}\right)_{max}\left(\frac{dw}{dt}\right)_{mean}}{T_i^2 T_b} \quad (3)$$

$$D_W = \frac{\left(\frac{dw}{dt}\right)_{max}}{T_i T_b} \quad (4)$$

where, $(dw/dt)_{max}$ is the maximum rate of mass loss (%·min^{-1}), $(dw/dt)_{mean}$ is the mean rate of mass loss (%·min^{-1}), t_i is the ignition time (min), t_p is the peak time (min), $t_{1/2}$ is the time span of $(dw/dt)/(dw/dt)_{max} = 1/2$, t_b is the burnout time (min), T_i is the ignition temperature (°C), and T_b is the burnout temperature (°C).

Kinetic analysis

The change of activation energy under different reaction conditions was analyzed by kinetic calculations, and then the difficulty of the reaction under different reaction conditions was judged according to energy variation. In isothermal thermogravimetric experiments, the reaction rate can be expressed according to the law of mass action[24]:

$$\frac{d(\alpha)}{dt} = k(T) f(\alpha) \quad (5)$$

where, t is the reaction temperature, $f(\alpha)$ is the reaction mechanism function, $k(T)$ is Arrhenius equation, and α is the sample conversion rate at time t.

$$\alpha = \frac{m_i - m_t}{m_i - m_f} \quad (6)$$

where, m_i is the initial mass of the sample, m_t is the instantaneous mass at time t, and m_f is the final mass of the sample.

$$k(T) = A\exp\left(\frac{-E}{RT}\right) \quad (7)$$

where, T is the reaction temperature, A represents the pre-exponential factor, E stands for the apparent activation energy, and R is the gas constant.

The heating rate: β (β = dT/dt) was substituted into the above equations to obtain the following:

Table 1 Proximate and ultimate analyses and lower heating value of the BC

Sample	Proximate analysis (Air dry basis, wt%)				Ultimate analysis (Air dry basis, wt%)					LHV (kJ·kg^{-1})
	M_{ad}	A_{ad}	V_{ad}	FC_{ad}*	C_{ad}	H_{ad}	O_{ad}*	N_{ad}	S_{ad}	
BC	5.97	24.42	20.25	49.36	61.34	1.65	5.31	0.67	0.64	24,675

M: moisture; A: ash yield; VM: volatile matter; FC: fixed carbon; LHV: lower heating value; *: calculated by subtraction.

Table 2 The quality of OCW

pH	COD (Cr) (mg·L^{-1})	Fe (mg·L^{-1})	Na (mg·L^{-1})	Cl (mg·L^{-1})	NH_3-N (mg·L^{-1})	TDS (mg·L^{-1})	Color
9.35	55,097	6,783	10,557	12.98	5,068.75	38,380	Aubergine

https://doi.org/10.48130/een-0026-0012

$$\frac{d\alpha}{dT} = \frac{A}{\beta}\exp\left(-\frac{E}{RT}\right)f(\alpha) \quad (8)$$

The function can be described by Eq. (5).

$$f(\alpha) = 1-\alpha \quad (9)$$

Model-free kinetic methods calculate Arrhenius parameters without selecting the reaction order. This approach adheres to the constant conversion rate method, where the reaction rate depends solely on temperature at a given conversion rate.

$$G(\alpha) = \int_0^\alpha \frac{d\alpha}{f(\alpha)} = \frac{A}{\beta}\int_{T_0}^{T}\exp\left(-\frac{E}{RT}\right)dT \quad (10)$$

After rearranging Eq. (8) using the Doyle approximation method, Eq. (11) for the Flynn–Wall–Ozawa (FWO) kinetic model is given as follows.

$$\ln\beta = \ln\left[\frac{AE}{RG(\alpha)}\right] - 5.331 - 1.052\frac{E}{RT} \quad (11)$$

The determination of activation energy, as demonstrated through the Kissinger–Akahira–Sunose (KAS) model, is illustrated in Eq. (12).

$$\ln\left(\frac{\beta}{T^2}\right) = \ln\left[\frac{AR}{EG(\alpha)}\right] - \frac{E}{RT} \quad (12)$$

Results and discussion

Thermogravimetry analysis

TG and DTG curves of BC and coal–OCW blends with different OCW mass fractions (1, 3, 5, and 10 wt%) during combustion at heating rate of 20 °C·min^{-1} are shown in Fig. 1. All the samples present a single main mass loss stage between 400 and 650 °C, which corresponds to the main combustion stage cuased by the oxidation of the volatile matter and fixed carbon. The DTG curves present similar peak characteristics, with the maximum mass loss rate of all samples occurring within the temperature range of 550–580 °C. However, as the OCW proportion increased, the maximum weight loss rate showed a slight decrease from 9.38 to 7.89%·min^{-1}, while the average weight loss rate also decreased from 5.05 to 4.41%·min^{-1}. This indicates that adding OCW leads to a certain reduction in the combustion intensity of coal. This can be attributed to the high moisture and organic acid content of the waste, which introduces additional endothermic decomposition reactions and increases the oxygen-deficient environment during devolatilization[24,25]. The peak temperature of the weight loss rate showed little variation among samples with different additive ratios, all occurring around 525 °C. The TG curves of the mixed samples exhibit a marginally greater residual mass in comparison to pure coal (BC100), ranging from 21.65% to around 25.17%. This suggests that the integration of OCW slightly amplifies the generation of inorganic residues.

Figure 2 illustrates the TG and DTG curves of the BC95OCW5 blend obtained at different heating rates (10, 20, and 40 °C·min^{-1}). As the heating rate increased from 10 to 40 °C·min^{-1}, T_p rose from 496.41 to 565.48 °C. Concurrently, $(dw/dt)_{max}$ increased from 4.60 to 17.21%·min^{-1}. With the increasing heating rate from 10 to 40 °C·min^{-1}, the TG curves gradually shift toward higher temperatures, and the main combustion stage becomes broader. This behavior mainly stems from the enhanced thermal lag effect under rapid heating conditions and the limited heat transfer process, resulting in a delay in the starting time of decomposition and combustion[26]. The dynamic compensation effect further amplifies this displacement by accelerating the reaction rate and shortening the reaction time at all temperatures. Therefore, the combustion process occurs in a broader temperature range. Correspondingly, the DTG peak of dynamic thermogravimetric analysis migrates to the high-temperature zone and the peak intensity is enhanced, indicating that the substance shows higher appearance reaction activity and faster mass loss rate[27].

Characteristic temperatures of samples at different heating rates are shown in Table 3. At all heating rates, with the increase of the heating rate, the characteristic parameters of coal combustion tend to develop to higher temperatures. This trend coincides with the thermal lag observed in the thermogravimetric analysis. When the heating rate accelerates from 10 to 40 °C·min^{-1}, T_i, T_p, and T_b of the sample increase obviously, and the maximum mass loss rate and average mass loss rate also increase synchronously. When OCW blends with coal for combustion, the combustion characteristics change significantly. Adding a small amount of OCW (1%–5%) can significantly reduce the ignition temperature, especially at a heating rate of 10 °C·min^{-1}. In fact, T_i was found to be approximately 15–25 °C lower than that of raw coal (BC100). This indicates that the organic components and metal ions such as Na and Fe present in OCW have a catalytic promoting effect, which can promote the initial oxidation reaction of fuel and improve its combustion characteristics[28,29]. OCW-derived Fe and Na species transform into Fe_2O_3, Fe_3O_4, Na_2CO_3, and Na_2O, which participate in redox cycles

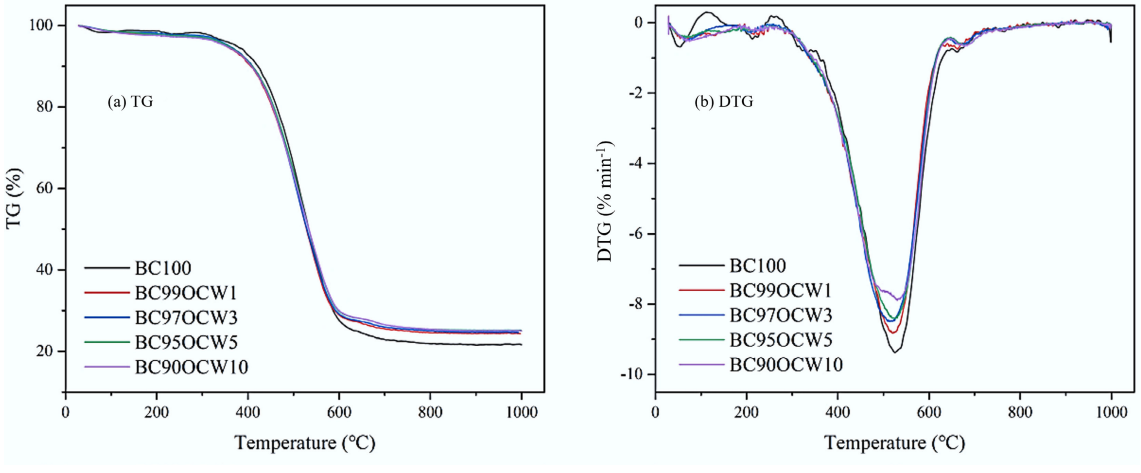

Fig. 1 TG and DTG curves of BC and OCW/BC blends during the combustion at 20 °C·min^{-1}: (**a**) TG, (**b**) DTG.

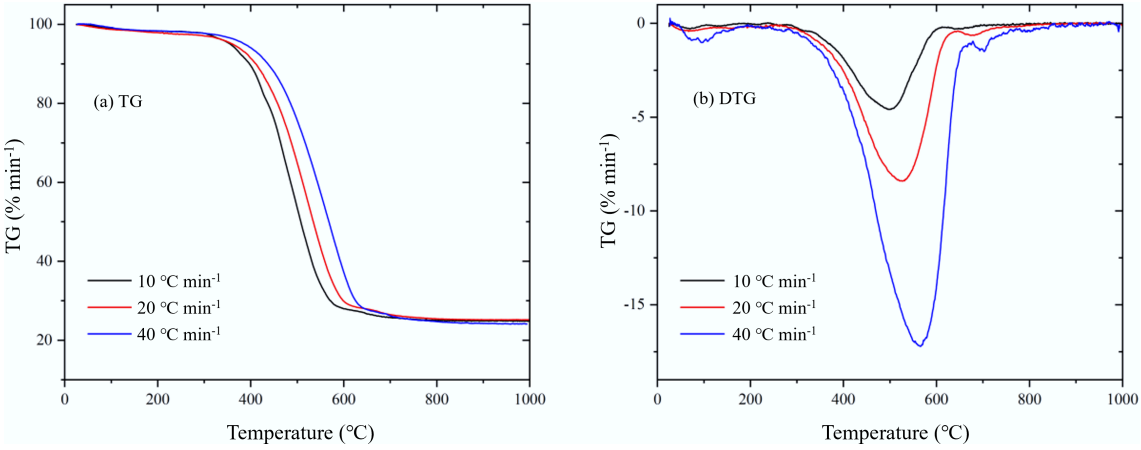

Fig. 2 TG and DTG curves of BC95OCW5 blends at different heating rates (10, 20, and 40 °C·min^{-1}): (**a**) TG, (**b**) DTG.

and promote the decomposition of oxygen-containing functional groups, resulting in enhanced char oxidation and lower activation energies at moderate OCW ratios.

Conversely, T_p does not change significantly, indicating that the influence of OCW is mainly concentrated on the initial volatilization and ignition stages of the volatile matter, with minimal impact on the main combustion stage. When the heating rate is 10 °C·min^{-1}, T_p is between 483.55 and 498.41 °C; when the heating rate is 20 °C·min^{-1}, T_p is between 521.53 and 528.06 °C; when the heating rate is 40 °C·min^{-1}, and T_p is between 556.63 and 565.48 °C.

T_b slightly decreases at a lower heating rate, suggesting a heightened degree of burnout and more thorough combustion. When the heating rate is 10 °C·min^{-1}, T_b of the sample with added OCW decreases from 674.64 to 654.25 °C, but when the heating rate is 20 and 40 °C·min^{-1}, T_b of the samples with added OCW increases from 688.24 and 708.48 °C to 697.42 and 722.45 °C, respectively. This might be due to the formation of a dense ash crust structure during combustion, which hinders oxygen diffusion as well as heat and mass transfer, thereby delaying the burnout reaction.

Table 3 Characteristic temperatures of samples at different heating rates (10, 20, and 40 °C·min^{-1})

Sample	B (°C·min^{-1})	T_i (°C)	T_p (°C)	T_b (°C)	$(dw/dt)_{max}$ (%·min^{-1})	$(dw/dt)_{mean}$ (%·min^{-1})
BC100	10	411.58	496.05	674.64	4.74	2.28
BC99 OCW1		390.56	483.55	645.80	4.30	2.06
BC97 OCW3		398.09	498.41	665.33	4.83	2.43
BC95 OCW5		396.76	496.41	664.83	4.60	2.36
BC90 OCW10		393.16	485.60	654.25	4.26	2.37
BC100	20	425.75	525.14	688.24	9.38	5.05
BC99 OCW1		425.34	521.53	679.54	8.83	4.80
BC97 OCW3		419.06	521.59	694.13	8.50	4.42
BC95 OCW5		427.91	526.87	691.87	8.41	4.54
BC90 OCW10		421.81	528.06	697.42	7.89	4.41
BC100	40	461.54	559.88	708.48	18.43	10.22
BC99 OCW1		451.37	556.63	711.08	18.34	10.02
BC97 OCW3		453.72	559.60	714.58	18.26	9.86
BC95 OCW5		432.33	565.48	721.58	17.21	9.21
BC90 OCW10		445.15	558.67	722.45	17.24	9.12

Furthermore, as the OCW content increases, both the $(dw/dt)_{max}$ and $(dw/dt)_{mean}$ exhibit a slight decrease. This shows that the combustion process has become relatively gentle. This may be due to the fact that the moisture and organic acids in the organic sludge absorb heat during decomposition, which weakens the heat conduction efficiency of the system and thus reduces the combustion rate.

As illustrated in Fig. 3, the comprehensive combustion indices (C_i, C_b, S, and D_w) exhibit clear and systematic variations with both the OCW blending ratio and the imposed heating rate. Overall, all indices decrease gradually as the OCW proportion increases from BC100 to BC90OCW10, demonstrating that the introduction of OCW imposes a suppressive effect on the combustion reactivity of the blended fuels. This is not only because OCW contains high levels of moisture and ash, which reduce the proportion of combustible material, but also due to the combined effects of multiple thermodynamic and kinetic processes.

C_i is a key parameter for comprehensively evaluating the ease of fuel ignition. A higher value indicates that the fuel ignites more readily and exhibits stronger initial reactivity. At a heating rate of 10 °C·min^{-1}, C_i remained around 2.6 × 10^3 %·min^{-3} with no significant change. The addition of OCW has little effect on coal ignition. However, when the heating rates increased to 20 and 40 °C·min^{-1}, C_i decreased from 1.81 × 10^3 and 1.17 × 10^4 %·min^{-3} to 1.53 × 10^3 and 1.14 × 10^4 %·min^{-3}, representing reductions of 15.5% and 2.56%, respectively. At higher heating rates, the ignition characteristics of coal deteriorate as the OCW dosage increases.

C_b is used to characterize the burnout performance of a fuel during the final stage of combustion, with higher values indicating a stronger tendency for complete combustion and better late-stage reactivity. When the heating rate is 10 °C·min^{-1}, C_b decreases from 1.2 × 10^{-4} to 9.5 × 10^{-5} %·min^{-4}. At a heating rate of 20 °C·min^{-1}, C_b decreased from 1.51 × 10^{-3} to 1.1 × 10^{-3} %·min^{-4}. At a heating rate of 40 °C·min^{-1}, C_b decreased from 2.07 × 10^{-2} to 1.83 × 10^{-2} %·min^{-4}. As OCW content increases, C_b shows a decreasing trend, indicating that adding OCW weakens the reactivity of coal during the later combustion stages.

S is one of the core parameters for evaluating overall combustion reactivity. A higher value indicates superior reactivity throughout the entire process from ignition to burnout. At 10 °C·min^{-1}, the addition of 1% OCW caused S to decrease slightly from 9.5 × 10^{-8} to

https://doi.org/10.48130/een-0026-0012

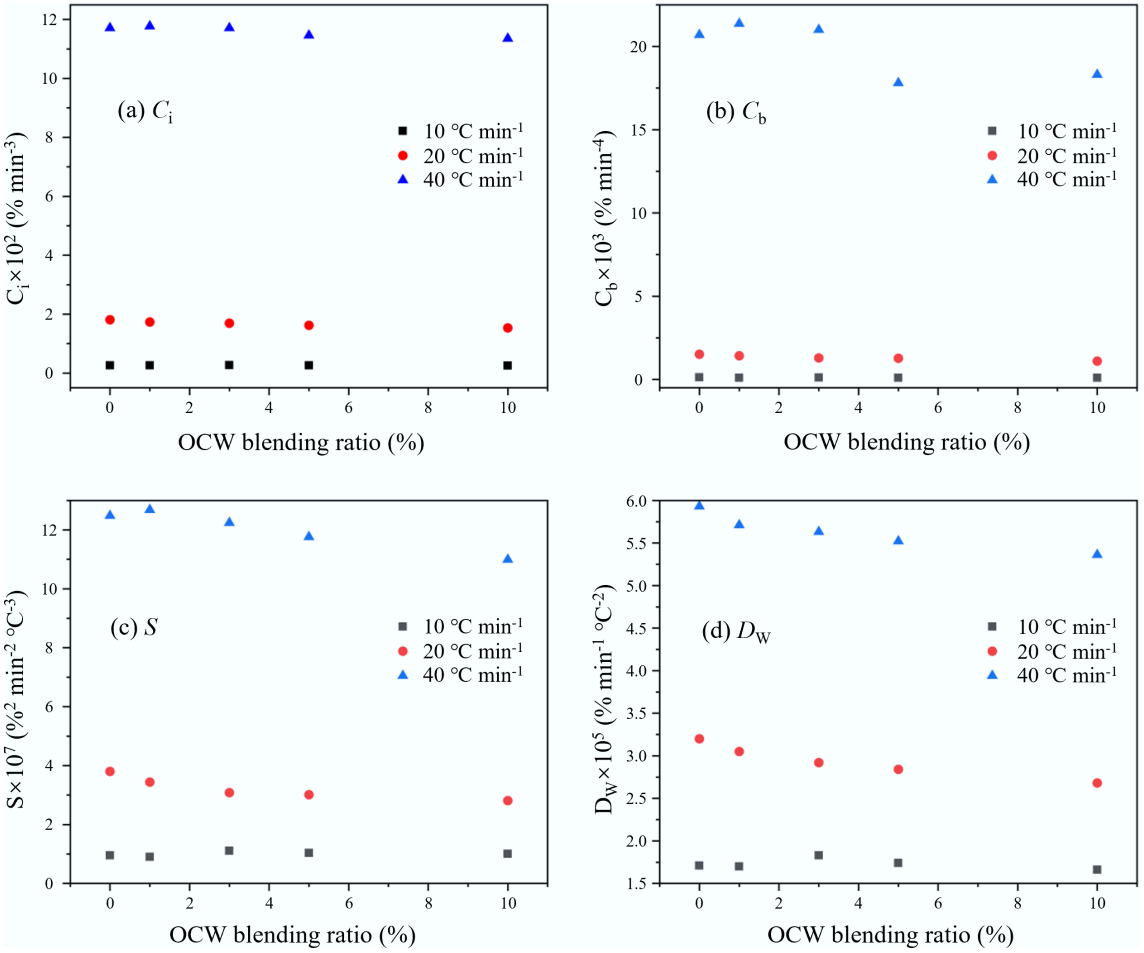

Fig. 3 Combustion characteristic indices for coal–OCW blends: (**a**) C_i, (**b**) C_b, (**c**) S, and (**d**) D_w.

9.0×10^{-8} %²·min⁻²·°C⁻³, indicating a minor reduction in overall combustion reactivity. However, when 3% OCW was blended, S increased to 1.11×10^{-7} %²·min⁻²·°C⁻³, suggesting that an appropriate amount of OCW may enhance the combined ignition and burnout performance due to the catalytic effects of its organic components and metal ions. As the blending ratio further increased to 5%–10%, S decreased to 1.03×10^{-7} and 1.00×10^{-7} %²·min⁻²·°C⁻³, respectively. At 20 °C·min⁻¹, S exhibited a continuous decreasing trend with increasing OCW content, dropping from 3.80×10^{-7} %²·min⁻²·°C⁻³ for raw coal to 3.44×10^{-7}, 3.08×10^{-7}, 3.01×10^{-7}, and 2.81×10^{-7} %²·min⁻²·°C⁻³, respectively, indicating that the adverse effects of OCW become more pronounced at higher heating rates, thereby reducing combustion integrity. At 40 °C·min⁻¹, S exhibited the highest overall value due to strong thermal feedback, yet still showed a decreasing trend with increasing OCW content. S increased from 1.25×10^{-6} %²·min⁻²·°C⁻³ in BC100 to 1.27×10^{-6} %²·min⁻²·°C⁻³ at 1% OCW, then decreased to 1.22×10^{-6}, 1.18×10^{-6}, and 1.10×10^{-6} %²·min⁻²·°C⁻³ at 3%–10% OCW. This indicates that a small amount of OCW may still have a promoting effect at high heating rates, but high OCW content significantly degrades combustion performance.

D_w reflects a fuel's ability to maintain a stable combustion rate under temperature variations, exhibiting distinct trends with changes in heating rate and OCW addition ratio. At 10 °C·min⁻¹, when the OCW blending ratio was 3%, D_w increased from 1.71×10^{-5} to 1.83×10^{-5} %·min⁻¹·°C⁻², indicating enhanced combustion stability of the coal. However, when the OCW content increased to 5% and 10%, D_w decreased to 1.74×10^{-5} and 1.66×10^{-5} %·min⁻¹·°C⁻², respectively. At 20 °C·min⁻¹, D_w monotonically decreased with increasing OCW blending ratio, from 3.20×10^{-5} %·min⁻¹·°C⁻² for raw coal to 3.05×10^{-5}, 2.92×10^{-5}, 2.84×10^{-5}, and 2.68×10^{-5} %·min⁻¹·°C⁻², respectively. This indicates that the adverse effects of OCW become more pronounced at higher heating rates. At 40 °C·min⁻¹, the D_w values for all samples reached their overall maximum but still exhibited a decreasing trend with increasing OCW content, decreasing from 5.93×10^{-5} %·min⁻¹·°C⁻² for BC100 to 5.71×10^{-5}, 5.63×10^{-5}, 5.52×10^{-5}, and 5.36×10^{-5} %·min⁻¹·°C⁻², respectively. This indicates that even under high thermal intensity conditions, excessive OCW still compromises combustion stability due to ash accumulation and combustible dilution.

The lower heating rate limits the rate of volatilization and oxidation, preventing the full manifestation of the inhibitory effect introduced by OCW. When the heating rate reaches 20 °C·min⁻¹, the release of volatile parts and the reaction of oxidation accelerate, thus enhancing the inhibitory effect of OCW on coal combustion. When the heating rate reaches 40 °C·min⁻¹, the strong thermal shock caused by rapid heating significantly increases the volatile release rate and coke oxidation rate, thus weakening the thermal dilution effect caused by organic carbon and the relative contribution of mass transfer restrictions in the overall reaction.

Thermokinetics analysis

In practical applications, the OCW addition ratio is usually about 5%, so 5% was selected as the representative condition. A 10% ratio was further used to examine the effect of higher OCW addition on coal combustion. The *E* values for BC100, BC95OCW5, and BC90OCW10 were determined using the FWO and KAS methods, with results shown in Figs 4–6. The activation energies obtained from the FWO model were slightly higher than those from the KAS model, consistent with the theoretical differences between the two methods.

For BC100, both models exhibit excellent linear correlation (R^2 > 0.99). When the conversion rate ranges from 0.1 to 0.7, the activation energy remains largely unchanged (≈130 kJ·mol^{-1}), indicating that initial combustion is primarily governed by the decomposition of stable carbonaceous structures. When α exceeds 0.7, *E* rose sharply to 163.1 kJ·mol^{-1}, reflecting a significant increase in the difficulty of oxidizing residual carbon.

For BC95OCW5, except when α = 0.1, where R^2 is approximately 0.87, R^2 exceeds 0.96 for all other conversion rates. This indicates that the addition of 5% OCW primarily influences the initial stages of coal combustion. As α increases, *E* rises from 106.8 to 136.2 kJ·mol^{-1}, yet remains relatively stable within the range of 115–120 kJ·mol^{-1} during the main combustion phase (α = 0.3–0.7), indicating a more uniform combustion process.

For BC90OCW10, α values exceed 0.95 across the board, whilst exhibiting a slightly elevated *E* value (≈136 kJ·mol^{-1}) during the initial stage. This may be attributable to an inhibitory effect from inorganic constituents or ash content present in the OCW. However, during the main combustion phase, the *E* value stabilised around 120 kJ·mol^{-1}, exhibiting only a slight increase at high α values. This indicates that excess OCW reduces combustion efficiency during the final oxidation stage.

The average activation energies are ranked as follows: BC100 (131.68 kJ·mol^{-1}) > BC90OCW10 (122.77 kJ·mol^{-1}) > BC95OCW5 (115.92 kJ·mol^{-1}), indicating that within the tested range, a moderate OCW blending ratio (5 wt%) provides a comparatively favorable balance of combustion reactivity and stability under the present experimental conditions. The reduction in *E* values can be attributed to oxygen-containing functional groups and volatile organic compounds present in OCW, which generate reactive free radicals and accelerate oxidation reactions. However, excessive addition of organic wastewater (10%) introduces increased ash and inorganic matter, potentially coating carbon surfaces and impeding oxygen diffusion, resulting in a slight rise in *E* values. Overall, both the FWO and KAS models confirm that adding organic wastewater reduces activation energy and promotes combustion.

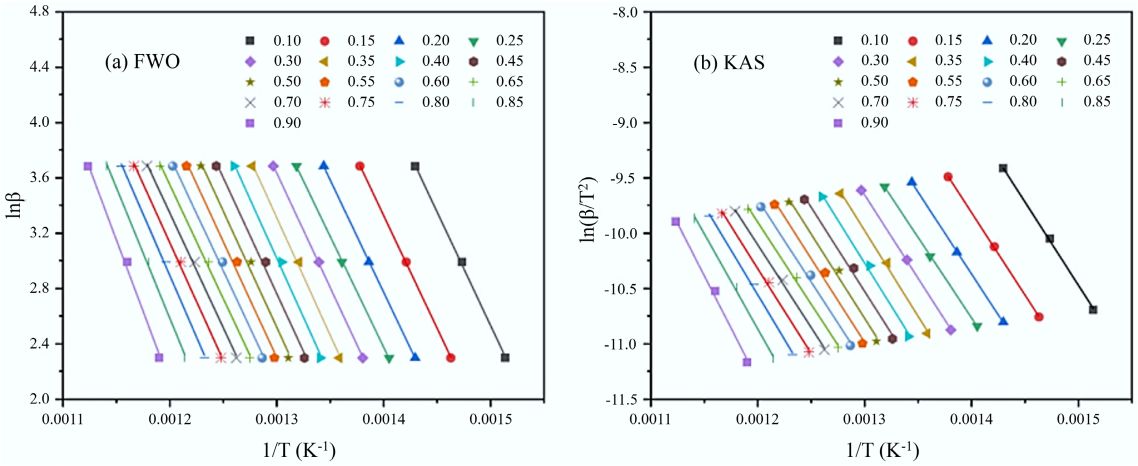

Fig. 4 Activation energy evaluation of BC100: (**a**) FWO, (**b**) KAS.

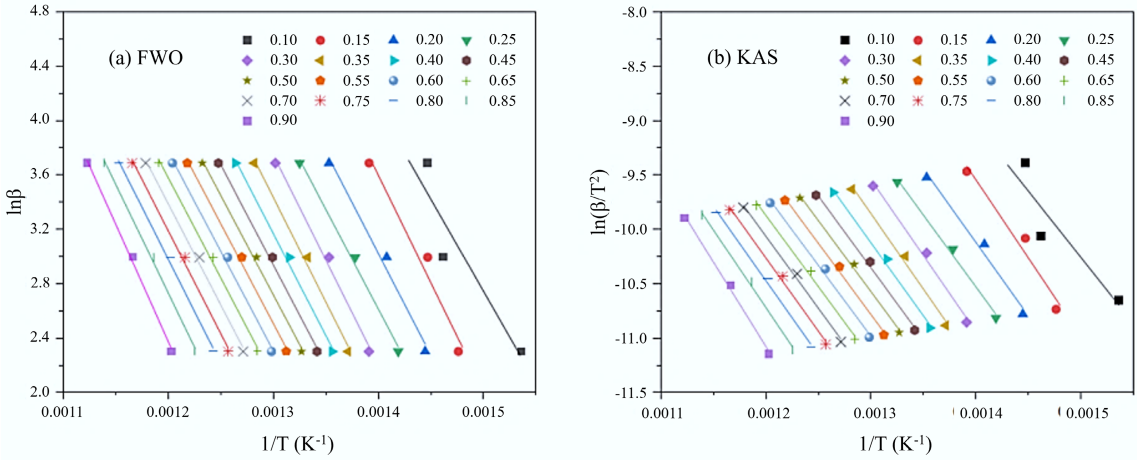

Fig. 5 Activation energy evaluation of BC95OCW5: (**a**) FWO, (**b**) KAS.

https://doi.org/10.48130/een-0026-0012

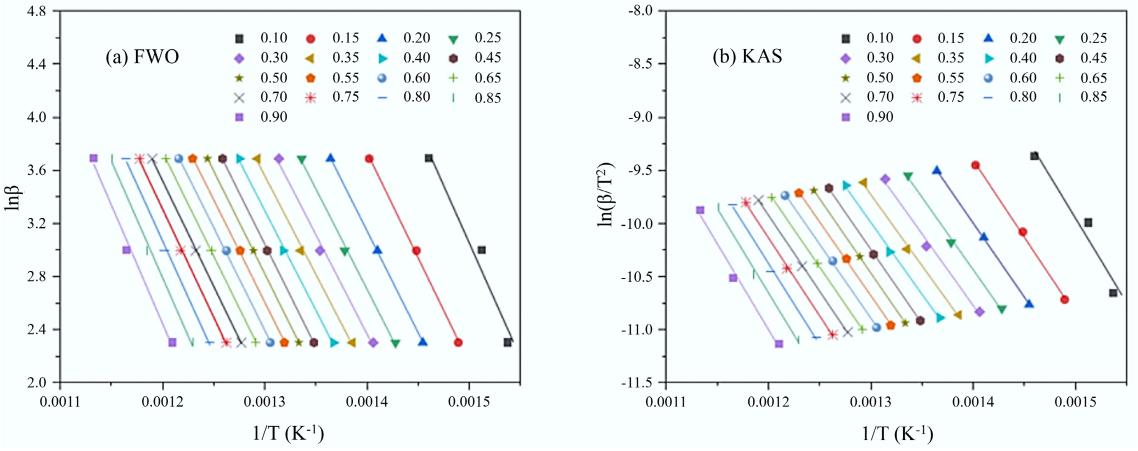

Fig. 6 Activation energy evaluation of BC90OCW10: (**a**) FWO, (**b**) KAS.

Conclusions

Moderate OCW addition altered the combustion behavior of bituminous coal through competing catalytic and inhibitory effects. At low OCW ratios, ignition was facilitated, whereas excessive OCW loading weakened overall combustion intensity and delayed burnout.

The observed behavior results from the balance between catalytic promotion by oxygen-containing organics and Fe/Na species and inhibition caused by moisture-induced heat absorption, combustible dilution, and ash-related diffusion resistance.

The isoconversional kinetic analysis shows that moderate OCW addition lowers the apparent activation energy, while excessive addition weakens late-stage oxidation. Under the present experimental conditions, a moderate blending ratio provided the balance between kinetic enhancement and combustion stability.

Author contributions

The authors confirm their contributions to the paper as follows: Jun Zhang: writing – review & editing, writing – original draft, validation, methodology, investigation, formal analysis. Yaji Huang: supervision, project administration, funding acquisition. Yizhuo Qiu: investigation, formal analysis. Xinyi Jiang: validation, formal analysis. Lanpeng Zhang: validation, formal analysis. Hao Shi: resources. All authors reviewed the results and approved the final version of the manuscript.

Data availability

The datasets generated during and/or analyzed during the current study are available from the corresponding author on reasonable request.

Funding

Funding was provided by the National Natural Science Foundation of China (Grant No. 52476108).

Declarations

Competing interests

The authors declare that they have no known competing financial interests or personal relationships that could have appeared to influence the work reported in this paper.

Author details

Key Laboratory of Energy Thermal Conversion and Control of Ministry of Education, School of Energy and Environment, Southeast University, Nanjing 210096, China

References

[1] Shams El Din AM, Tag El Din AMK. 1989. Electrochemical monitoring of the process of boiler cleaning. *Desalination* 75:171–184

[2] Zhao X, Huang Z, Sun H, Zhao Q, Huang Z, et al. 2024. Comparison on molecular transformation of dissolved organic matter during Fenton and activated carbon adsorption processes for chemical cleaning wastewater treatment. *Separation and Purification Technology* 344:127226

[3] Tong J, Zhu Z, Yang Y, Jiang Y. 2021. Removal of chemical oxygen demand from ethylenediaminetetraacetic acid cleaning wastewater with electrochemical treatment. *Separation and Purification Technology* 267:118651

[4] Zhang Y, Sun X, Wang F, Su T, Yang S, et al. 2024. Study on the effect and regularity of plating parts cleaning wastewater by enhanced aerobic process with high-density bacterial flora. *Journal of Environmental Management* 357:120653

[5] Poelmans S, Nagels M, Mignot M, Dewil R, Cabooter D, et al. 2023. Application of partial ozonation on tank truck cleaning concentrate and the influence on biodegradability and ecotoxicity: a pilot-scale study. *Water Science and Technology* 87:1–12

[6] Nagels M, Poelmans S, Dries J, Lambert N, Van Aken P, et al. 2021. Pilot-scale evaluation of ozone as a polishing step for the removal of nonylphenol from tank truck cleaning wastewater. *Journal of Environmental Management* 288:112396

[7] Gharaghani MA, Hashemi H, Samaei M, Ameli F, Bontempi E, et al. 2025. Assessing pollution levels and implementing eco-friendly hybrid sedimentation and sono-electrocoagulation for car wash wastewater treatment. *Physics and Chemistry of the Earth, Parts A/B/C* 140:103999

[8] Gusiatin MZ, Pasieczna-Patkowska S, Bálintová M, Kuśmierz M. 2023. Treatment of wastewater from soil washing with soluble humic substances using biochars and activated carbon. *Energies* 16:4311

[9] da Silva SW, Klauck CR, Siqueira MA, Bernardes AM. 2015. Degradation of the commercial surfactant nonylphenol ethoxylate by advanced oxidation processes. *Journal of Hazardous Materials* 282:241–248

[10] Senn AM, Russo YM, Litter MI. 2014. Treatment of wastewater from an alkaline cleaning solution by combined coagulation and photo-Fenton processes. *Separation and Purification Technology* 132:552–560

[11] Karci A, Arslan-Alaton I, Bekbolet M. 2013. Advanced oxidation of a commercially important nonionic surfactant: investigation of degradation products and toxicity. *Journal of Hazardous Materials* 263:275–282

[12] Zeng B, Jiang Y, Pan Z, Shen L, Lin H. 2023. Feasibility and optimization of a novel upflow denitrification reactor using denitrifying granular sludge for nitric acid pickling wastewater treatment. *Bioresource Technology* 384:129271

[13] Yuan L, Xu M, Xu R, Ji C, Yang H, et al. 2023. Insights into the adsorptive separation of iron from pickling waste acid: the overlooked role of $FeCl_3$ species. *Chemical Engineering Journal* 477:146637

[14] Yang X, Song G, Xiao Y, Ji Z, Wang C. 2022. Characteristics of pyrolytic wastewater incineration and effects on NO emissions of shenmu coal. *Journal of Environmental Chemical Engineering* 10:108041

[15] Ji Q, Tabassum S, Hena S, Silva CG, Yu G, et al. 2016. A review on the coal gasification wastewater treatment technologies: past, present and future outlook. *Journal of Cleaner Production* 126:38–55

[16] Mabrouk M, Marchand M, Russello A, Baronnet JM, Lemont F. 2015. Development of a submerged thermal plasma process for combustion of organic liquid waste. *Plasma Chemistry and Plasma Processing* 35:45–60

[17] Ma J, Feng S, Zhang Z, Wang Z, Kong W, et al. 2022. Effect of torrefaction pretreatment on the combustion characteristics of the biodried products derived from municipal organic wastes. *Energy* 239:122358

[18] Yang L, Zhang Z, Li F, Zha X, Mao W, et al. 2025. New insights on co-combustion of organic waste liquid blending with pulverized coal: synergistic effect on the combustion performance and pollutant control. *Fuel* 399:135629

[19] Zang C, Tang G. 1992. Incineration treatment of citric acid pickling waste liquid from boilers. *East China Electric Power* 1–5 (in Chinese)

[20] Chen H. 2013. Treatment of EDTA-containing chemical cleaning wastewater from power plants and its environmental impact analysis. *Guangdong Electric Power* 26:109–112 (in Chinese)

[21] Jiang P, Meng Y, Parvez AM, Dong XY, Wu XY, et al. 2021. Influence of co-processing of coal and oil shale on combustion characteristics, kinetics and ash fusion behaviour. *Energy* 216:119229

[22] Yang X, Hui S, Tang T, He Y, Wu H. 2025. Municipal solid waste management assisted by high-calorific-value industrial waste: co-combustion behaviors and pollutant emission. *Energy Sources, Part A: Recovery, Utilization, and Environmental Effects* 47:2532096

[23] Caliskan Sarikaya A, Haykiri Acma H, Yaman S. 2019. Synergistic interactions during cocombustion of lignite, biomass, and their chars. *Journal of Energy Resources Technology* 141:122203

[24] Li X, Jin Z, Bai G, Wang J, Linghu J. 2022. Experimental study of the influence of water on spontaneous combustion of coal containing pyrite. *International Journal of Coal Preparation and Utilization* 42:1357–1372

[25] Sun J, Yan L, Qin Y, Wang H, Xu Y, et al. 2025. Effect of extrinsic moisture on spontaneous combustion characteristics of water-immersed coal: an experimental study. *Combustion Science and Technology* 1–22

[26] Gao J, Chang M, Shen J. 2017. Comparison of bituminous coal apparent activation energy in different heating rates and oxygen concentrations based on thermo gravimetric analysis. *Journal of Thermal Analysis and Calorimetry* 130:1181–1189

[27] Hu Y, Wang Z, Cheng X, Ma C. 2018. Non-isothermal TGA study on the combustion reaction kinetics and mechanism of low-rank coal char. *RSC Advances* 8:22909–22916

[28] Song Y, Chen Y, Su S, Tang H, Han H, et al. 2022. Effects of inorganic sodium on the combustion characteristics of Zhundong coal with fast-heating rate. *Fuel* 319:123801

[29] Deng B, Qiao L, Wang Y, Mu X, Deng C, et al. 2023. Study on the effect of inorganic and organic sodium on coal spontaneous combustion. *Fuel* 353:129256